Fatigue Life Prediction of Titanium Implants with Titanium Dioxide Surface

ŠTĚPÁN MAJOR, MICHAL RŮŽIČKA, PAVEL CYRUS
Department of Technical Education, Faculty of Education
University Hradec Králové
Rokitanského 63, Hradec Králové 500 03
CZECH REPUBLIC
s.major@seznam.cz, michal.ruzicka@uhk.cz, pavel.cyrus@uhk.cz

Abstract: - Most of mechanical components in the engineering are frequently subjected to multi-axial loading, which also applies to medical engineering. The cyclic-loading can lead to sudden fatigue failure. In present work the fatigue life of cylindrical titanium components of dental implants made from titanium alloys 6Al-4V ELI and 6Al-7Nb were studied. Contrary to surface treatments used in industry, the main goal of titanium dioxide deposition is to improve implants biocompatibility. The effect of surface treatment on fatigue life of implant was tested experimentally. Two sets of experimental samples differed in surface layer thickness, so that its influence can be compared. Its fatigue behaviour was studied and predictive models were tested. Sixteen different models were applied and analysed in order to obtain the best way to predict fatigue life of implant. Two different types of implants were tested. First type of implant uses abutment screw to fix the crown. This type has four parts. Second type of dental replacement has only three components. This type utilizes abutment polygonal thorn to fix the crown. Experiments show that, the effect of titanium dioxide surfaces on implants mechanical properties is considered negligible. Therefore implants fatigue life is not dependent on dioxide layer thickness. The Gonçalves- Araujo- Mamiya criterion was found the best in implants fatigue prediction. The prediction of fatigue life of polygonal thorn is more complicated, so its prediction is gives inferior results contrary to the first type of implant.

Key-Words: - Fatigue testing, Bending-torsion loading, Titanium dioxide, Biocompatibile surface, Dental replacement, abutment screw.

1 Introduction

It is well known that components subjected to the repeated loading will fail after a certain number of cycles. This will happen even in the case that loading amplitude is deep below ultimate tensile stress, respectively below yield stress. The fatigue degradation can be described as progressive and localized structural [1,2,3,4]. Microscopic cracks will begin to form at the surface when the local value of above a certain threshold. This happens in places where the stress concentrators are present, i.e. in the corners and at the sharp edges or in places where material defects occur. These material defects can be often connected with fault thermal treatment or surface deposition. When local crack was generated, it will be growing and after some time will reach a critical size, and the structure will suddenly fracture.

As has already been said, the nominal maximum stress values are less than the yield stress limit of the metals. Fatigue failure occurs when a material is repeatedly subjected to external forces. This loading force is not necessarily described by periodic function, i.e loading is not described by periodic function such as sine function and others.

An example of such non-periodic loading can be a dental implant [5]. The dental implant consists of three or four main parts [5]. These components are: ceramic crown that is attached to the thorn or abutment screw and cylindrical housing. This abutment thorn or screw is inserted in the housing box, which is ingrown in the bone of the jaw. The abutment thorn has shape of conical thread or polygonal prism. The housing box (often called fixture) has internal cavity which serves to fasten the bolt or polygonal horn. This cavity has an internal thread or its cross-section is polygonal in the case of using polygonal thorn. Similar component as housing box in the jaw is often part of ceramic crown and this component serve to fast the thorn and the crown. It should be recounted, that most often solution is based on combination both approaches. The bottom section of thorn is a screw

and its upper section is polygon (this section is mostly shorter than bottom section of thorn, see Fig.1). In some cases the abutment is another part of assembly. The abutment can be straight (this is a common form) or angled. An angled abutment is used for replacement of aslant growing teeth in the case that the implant must hold same slope as surrounding teeth.

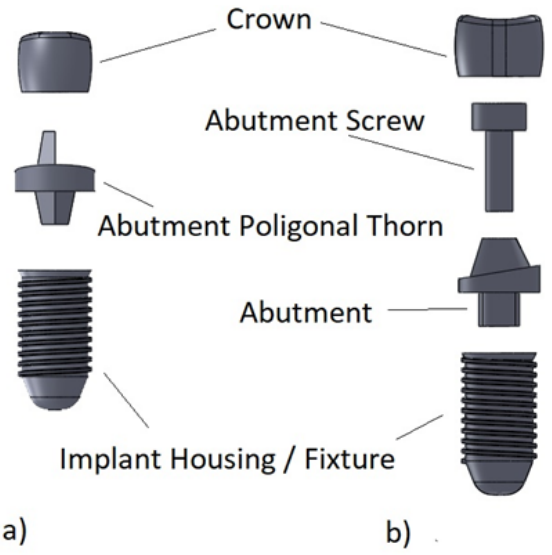

Fig. 1 Dental implants: a) Implant with abutment thorn; b) Implant with abutment and abutment screw.

In this article we the biological causes of the implant failure are not analysed. Therefore, here is only a brief mention about reasons for the body rejection of implant as a foreign body. This process can be associated with various inflammations and other diseases [5,7,8]. This paper is devout only to mechanical causes of the implant failure, respectively to fatigue failure of a threaded or thorn caused by repeated forces. The thorn with thread can be considered as an example of cylindrical or conical sample with notch under bending- torsion loading.

2 Material of implants

Majority of metal components used in dental implantology [5,6,7,8] are manufactured from titanium alloys. Arguably, the most appropriate titanium alloys used in medicine are 6Al-4V ELI alloy and 6Al-7Nb alloy. The abbreviation ELI in denomination of the first alloy means Extra-Low Interstitials. Thus, titanium alloy 6Al-4V ELI is characterized by very low content of interstitial atoms. The main reason for reduce the concentration of interstitial atoms is that these atoms diffuse in the body. The interstitial atoms of vanadium are considered as harmful and carcinogen or cytotoxic.

The titanium alloy 6Al-4V ELI (ASTM standard: Grade 23 alloy) is very close to the titanium alloy 6Al-4V (ASTM standard: Grade 5 alloy), which is intended for industry and its mechanical properties are practically the same. The mechanical properties of titanium alloy 6Al-4V ELI are: Elastic modulus E = 113.8 MPa, ultimate strength $\sigma_u = 893$ MPa, yield stress $\sigma_y = 827$ MPa, crack growth properties are characterised by constants $C = 7.8 \cdot 10^{-14}$ and $m = 4.9$. These two constant are known from the Paris-Erdogan law. Crack growth properties were measured according to ASTM E647 [9].

The titanium alloy 6Al-7Nb (ASTM standard: ASTM F 1295) was especially developed for medical use as alternative for 6Al-4V alloy. The mechanical properties of titanium alloy 6Al-4V ELI are: Elastic modulus E = 112 MPa, ultimate strength $\sigma_u = 895$ MPa, yield stress $\sigma_y = 819$ MPa, crack growth properties are characterised by constants $C = 6.4 \cdot 10^{-13}$ and $m = 8.2$.

3 Surface Treatment of Implants

One of the most common ways to improve components resistance to the external influences is modification of components surface. By changing surface layer properties of machinery parts it is possible to increase both corrosion resistance and their load-capacity. In case of medical engineering, the first task of surface layer deposition is upgrading of biocompatibility [5,6,7,8].The metallic alloy of which dental replacement is made, can release harmful particles in the patient body. Release of these particles can be explained by corrosion. This corrosion is caused by implants contact with body fluids. Another important factor in implants failure is deposition of biological sediments on the implant surface. Therefore, self-cleaning is one of the most important properties of biocompatible surfaces.

The preferred surface treatment is titanium dioxide deposition [7,8]. The titanium dioxide surface is an example of nano-surface and its self-cleaning feature significantly increases the likelihood, that the implant will be accepted by the human body.

In medical engineering ion-beam-assisted sputtering deposition technique has been used to

deposit thick and dense titanium dioxide films on titanium alloys and stainless steel surfaces [9]. The ion-beam-assisted sputtering deposition is combination of ion implantation with simultaneous sputtering or another physical vapour deposition technique. Configuration with sputter deposition is preferred. Sputtering is a physical vapour deposition, this technique involves ejecting material from "target" that is the source of source onto a "substrate". In the case of studied implants the distance between the target and the substrate was set at 15 cm and the base pressure in the plasma chamber was 0,01. Titanium content in target was 99.99%. This target was sputtered with plasma beam characterized by specific energy 14 $W.cm^{-2}$. The content of argon in the plasma beam was 99.99% and reactive oxygen was introduced between the plasma and the substrate. An appropriate selection of the oxygen flow was required. For this work, we prepared samples at temperature 400 °C and two deposition times, corresponding to equivalent film thicknesses of 5 nm and 20 nm. The deposition rates were determined by using a quartz crystal located in the deposition chamber near the substrate. The parameters of deposition process are same for both titanium alloys (6Al-4V ELI and 6Al-7Nb) used in the study.

Titanium 6Al-4V alloy is generally considered as a standard material when evaluating the fatigue resistance. However, the mechanical response of this alloy is extremely sensitive to prior thermo-mechanical processing [9]. The changes in the β grain size, the ratio of primary α phase transformed to β phase, the α grain size and the α/β morphologies, all this characteristics have grate impact on fatigue performance and mechanical properties of final product. Particularly high-cycle fatigue lifetime is heavily influenced. For example, maximum fracture toughness and fatigue crack growth resistance is achieved when Widmanstätten microstructure was achieved during heat treatment (annealing) [9]. In this case annealing is resulting β recrystallization. However, Widmanstätten microstructure leads to decline of fatigue resistance in the high cycle fatigue [9].

Therefore, specimens used in this study were processed to achieve development of a bi-modal primary α plus transformed β microstructure. In this manner probability of fatigue crack initiation was reduced [8,9]. In the case titanium alloy 6Al-7Nb is the effect of heat treatment less significant than in the case of 6Al-4V alloy.

The effect of dioxide surface on the fatigue resistance of implant is disputable. With regard to it and intensive cyclic loading of dental implant, it is necessarily study this problem.

4 Testing of Abutment Screw

The geometry of experimental sample is based on standard dental implant. The testing sample used different type of crown. This crown was made from steel. The testing machine can be described as rotating plate with holes and base with implant holder. These two plates are alternately in the opposite direction. Alternating impact forces caused bending of implant. The implant is fixed on the base plate of testing machine, schematic view is shown on Fig. 2. The testing device is constructed like that mutual inclination of axes of both plates is changeable. This solution allows control the intensity of the impact forces. The experiments were performed on four sets of specimen: (1) specimens with screw and titanium dioxide surface layer 5 nm; (2) specimens with screw and titanium dioxide surface layer 20 nm; (3) specimens with polygonal thorn and titanium dioxide surface layer 5 nm; (4) specimens with polygonal thorn and titanium dioxide surface layer 20 nm. Experimental sets (1) and (2) were performed on 15 specimens each. Experimental sets (3) and (4) had 10 and 8 sample respectively. The loading the implant can be described as effect of two external forces: first force bends specimen and the second force cased twist of specimen. The implant, respectively the abutment screw or thorn is under bending-torsion loading. However, the bending forces prevail over torsion forces. The loading can be characterized by ratio between burdening forces or even more appropriately between stress amplitudes r_L caused by this forces. This ratio can be defined as $r_L = \tau_a / (\tau_a + \sigma_a)$, where τ_a is amplitude of stress caused by torsion and σ_a is amplitude of stress caused by bending forces. In this test the value of ratio r_L is about 0.2. The fatigue test was performed to final rupture of specimen. The experiments were performed at the room temperature. The fatigue life N_f of investigated specimens was in the order from 10^3 to 10^5 cycles. The fatigue crack generated in the region of maximal value of stress/strain. In the case of abutment screw, the fatigue crack originated on the bottom of thread. If the polygonal abutment

thorn is used, the fatigue crack occurred on thorns tapering.

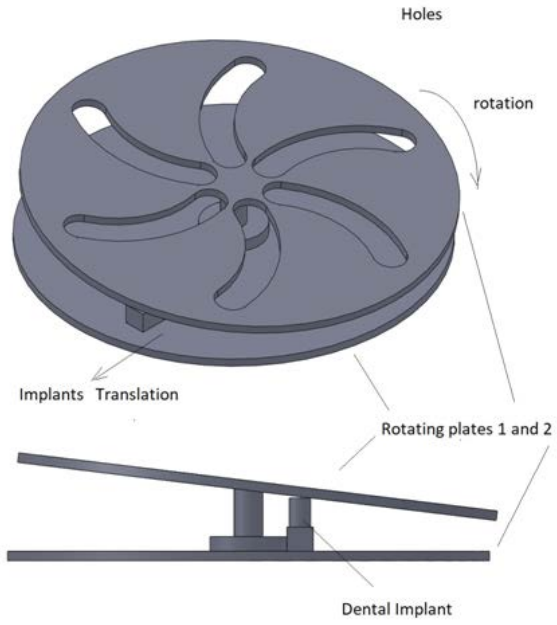

Fig.2 Fatigue testing- Principle of test machine. The plates are rotating and the implant can be shifted partially.

4 Fatigue Life Predictions

In practice majority of mechanical components in engineering practise is subjected to the bi-axial or tri-axial loading, eventually even more complicated cases. In general, the multi-axial loading can be described as combination of simple loading modes such as, torsion, bending or tension. This simple loading modes or forces could be described by mutually independent functions. These functions are often time dependent components of stress tensor. When the individual components of stress tensor are in-phase during the loading, the fatigue life is usually shorter than in case of out-of-phase loading

In most industrial laboratories, there are only basic fatigue testing machines available. These basic machines does not allow multi-axial test. Therefore, one of the most difficult tasks in fatigue fracture simulation is to translate the information gathered from uni-axial fatigue tests on engineering materials into applications involving complex states of cyclic stress-strain conditions.

Many approaches have been proposed for prediction of multi-axial fatigue life prediction. Fatigue life prediction is often based by this approach: (1) The stress (respectively strain) state of component under loading is described by its location in stress-strain space; (2) This space is divided in two parts. Boundary curve (in case of bi-axial loading) or surface (universally in the case of multi-axial loading) divide stress space the stress space to the safe and the unsafe region. However, the function defining the division of the space is not yet established. In addition to a stress-based approach, equally strain based approach is used. Further, we encounter more complex approaches, such as approach based on Ilyushin space. In addition to these methods, sometimes direct simulation of fatigue degradation is used, see [3,5,10,11,12,13,14,15,16,17]. However, this approach is not object of interest of this paper.

Let's start with the assumption, that the normal and shear stress components σ_a and τ_a, acting in a critical volume, control the fatigue life under combined bending-torsion loading. As far as, these components are known, the prediction of bi-axial fatigue life using data obtained by uni-axial tests is basically possible. As mentioned above, the stress space is divided to the safe and the unsafe parts by function or its value, which is called multi-axial fatigue criteria. The points bellow the boundary line lie in the safe region whereas the points above the line are in the unsafe region. The most general form of fatigue criteria can be written as an inequality:

$$a \cdot f(\tau_a) + b \cdot g(\sigma_a) \leq \sigma_c . \tag{1}$$

Where parameters *a* and *b* are limit values obtained from two uni-axial fatigue tests. Therefore, these two parameters corresponds to fatigue limit in fully reversed torsion τ_c and in tension σ_c). In some cases, the linear combination of shear stress τ_a and normal stress σ_a in Eq.1 can be replaced by a quadratic form.

In this paper sixteen classical and advanced multi-axial criteria were used to predict the fatigue life of dental implants. This approach was used to assess the prediction quality: (1) If the load data of the left–hand side of Eq.1 (further referred as an abbreviation *LHS*) correspond the to experimentally determined fatigue limit (right-hand side *RHS* of the inequality Eq.1), the ideal state of equality should be achieved. The accuracy of the fatigue life prediction by means of multi-axial criteria can be expressed by the so-called error index *I:*

$$I = \left(\frac{LHS - RHS}{RHS} \right) \cdot 100\% . \tag{2}$$

The error index expresses a percentage of deviation from the real fatigue life. The ideal prediction leads to equality *LHS* = *RHS*, i.e. I = 0. The positive value of the error index means, that the criterion yields conservative results, i.e. the real fatigue life of implant is higher than that predicted by criterion and, therefore, the predicted number of cycles N_f to implant failure lies on the safe side of the boundary line.

Scope of this article does not allow a deeper analysis of all the compared criteria. Therefore, only some of the selected criteria are discussed in paper. Criteria discussed in the paper were selected to represent certain approaches to solving the problem. Criteria can be divided between classical and advanced. These approaches are also distinguished: quadratic form of classical criterion, critical plane approach and integral approach, criteria based on Ilyushin space. As the examples of classical fatigue criteria were tested criteria proposed by Gough and Pollard, McDiarmid, Matake or Kakun-Kawado criteria [5]. As an example of integral approach were chosen two criteria: First Papadopoulos criteria and Keunmegna criteria. The criterion proposed by Gonçalves, Araujo and Mamiya is an example of criteria based on five-dimensional Ilyushin space. It is necessary to emphasize, that all criteria are adapted on the case notched specimen. Reason for this modification is a thread on the abutment. The thread is an example of notched specimen. These notches working as stress concentrators.

The Gough - Pollard criterion is considered as the oldest multi-axial criteria, because it was proposed in the thirties of the twentieth century. These two authors suggested an empirical ellipse formula as a multia-xial fatigue criterion [5]. This relationship is suitable for ductile materials:

$$\left(\frac{A_{GP}\sigma_a}{\sigma_c}\right)^2+\left(\frac{B_{GP}\tau_a}{\tau_c}\right)^2\le 1. \quad (3)$$

Parameters A_{GP} and B_{GP} were obtained by comparison of the Wőhler curves for notched and smooth specimens. Both parameters are equal 1 for smooth specimens.

In the case of brittle materials was proposed used modified Gough - Pollard criteria. This criterion is considered as preferable sample with stress concentrators [5]:

$$\left(\frac{A_B\sigma_a}{\sigma_c}\right)^2\left(C_B\kappa-1\right)+\frac{B_P\sigma_a}{\tau_c}\left(2-\kappa\right)+\frac{A_B\sigma_a}{\tau_c}\le 1. \quad (4)$$

Where κ is ratio of fatigue limit defined as $\kappa=\sigma_C/\tau_C$ and parameters A_B, B_B and C_B were obtained by same approach as in the previous case.

The McDiarmid [13,14] criterion is frequently used, because this criterion was implemented in commercial fatigue software such as MSC.Fatigue or FE-Fatigue. This author identifies damage parameter as maximum value of stress at the plane of maximum shear stress range. Damage is computed on this plane by combining the shear stress and normal stress. The McDiarmid criterion can be written according to convention defined by Eq. 1:

$$\frac{A_{MD}.\sigma_C.\tau_{a,\max}}{t_{A,B}}+\frac{B_{MD}\sigma_C}{2\sigma_U}\le C_{MD}\sigma_C. \quad (5)$$

Where, the σ_U is the ultimate strength. Parameters A_{MD}, B_{MD} and C_{MD} were obtained by comparison of the Wőhler curves for notched and smooth specimens. Subscript *a* mean amplitude and subscript *max* denotes maximum value of stress. The subscript *A,B* in this criterion represents choice between t_A a t_B fatigue limits corresponding to load conditions leading to cracks growing in two distinct directions: first system is parallel to the surface (A); second system is characterized by growth inwards from the surface (B). This distinction between two cracking systems is not usually defined. In the case of plane bending combined with torsion is generally fulfilled equality $t_{A,B} = \sigma_C$ [5,13,14].

The Matake criterion can be written as an inequality:

$$C_M a_M \tau_{a,MSSR}+D_M b_M \sigma_{\max,MSSR}\le A_M\sigma_c. \quad (6)$$

Subscript MSSR by normal shear stress is abbreviation of Maximum Shear Stress (or Strain) Range. This means that the critical plane was set according to Parameters a_M and b_M in this criteria are defined as $a_M = \kappa$ and $b_M = 2 - \kappa$. Variable κ is fatigue limits ratio $\kappa = \sigma_c/\tau_c$. Parameters A_M, C_M and D_M are equal to 1 for smooth specimen. These parameters were obtained by same manner as in the previous cases.

Crosland published his criterion already before fifty years. His original criterion was intended for smooth specimen. This criterion is utilizing

amplitude of the second invariant of stress tensor deviator. This deviator corresponds to the von Mises stress. If the notch is present, theoretically no adjustments are needed. Because, theoretically, we can assigned certain value of stress/strain tensor (or by its components) to each point in the implant should. Actually, some corrections are necessary. The Crosland criteria modified for sample with V notch (characterized by acute angle between groove faces) can be written:

$$A_C a_C \sqrt{J_{2,a}} + B_C b_C \sigma_{H,a} \le \tau_c . \quad (7)$$

Parameters a_C and b_C can be obtained through the evaluation of the formulas at fatigue limits in torsion and tension or bending. The appropriate values of material parameters are $a_C = \kappa$ and $b_C = 3-\sqrt{3}\kappa$. The parameters A_C, B_C are characterizing the influence of notch shape.

The Kakuna-Kawada criteria [5] can be written as:

$$a_K \sqrt{J_{2,a}} + b_K \sigma_{H,a} + c_K \sigma_{H,m} \le \tau_c . \quad (8)$$

Where, the $J_{2,a}$ is the second invariant of stress tensor deviator. The $\sigma_{H,a}$ and $\sigma_{H,m}$ are amplitude and mean value of hydrostatic stress. Parameters a_K, b_K and c_K are material parameters obtained from uni-axial fatigue test.

The Keunmegna Integral criterion based on integral approach is one example of advenced stress based kriteria [16]. This criterion can be expressed as:

$$\sqrt{\int_{\varphi=0}^{2\pi}\int_{\psi=0}^{\pi} \frac{\phi(\tau_a,\sigma_a,\sigma_m)}{4\pi.Q_{Ke}} \sin\psi d\psi d\varphi} \le \sigma_c . \quad (9)$$

Where, φ and ψ are Euler angles between the global coordinate system and the examined plane. The subscript m denotes mean value of stress. The function $\phi(\tau_a,\sigma_a,\sigma_m)$ in Eq.8 can be written as:

$$\phi(\tau_a,\sigma_a,\sigma_m) = A_{Ke} a_\kappa \tau_a + B_{Ke} b_\kappa \sigma_a + D_{Ke} d_\kappa \sigma_m . \quad (10)$$

Parameters A_{Ke}, B_{Ke}, D_{Ke} and Q_{Ke} represents correlation of elevation of local stress value caused by cross-sectional reduction at the bottom of thread. These parameters are functions of the notch profile. Parameters a_κ, b_κ and c_κ are material parameters.

The example of advanced stress based multi-axial criteria is Papadopoulos integral criterion [10,11,15]. In Papadopoulos criterion based on integral approach are both input variables (shear stress and normal stress) integrated over all planes [10,11,15]:

$$\sqrt{a_P \iiint T_a^2 d\chi \sin\psi d\psi d\varphi} + b_P \cdot \sigma_{H,\max} \le \sigma_c . \quad (11)$$

The variable $T_a = T_a(\varphi,\psi,\chi)$ is amplitude of resolved stress. Because, the resolved stress is function of Euler angles φ, ψ and χ, the amplitude of stress is identified by stress maximalization in all directions. The $\sigma_{H,,\max}$ is maximum value of hydrostatic stress. The parameters a_P and b_P are defined as:

$$a_P = \frac{5\kappa^2}{8\pi^2},\ b_P = 3-3\kappa . \quad (13)$$

Criterion proposed by trio Brazilian authors Gonçalves, Araujo and Mamiya is considered as very effective [18]. This criterion is utilizing a construction of minimum circumscribed ellipsoid over the load path in five-dimensional deviatoric Ilyushin space. This criterion can be expressed as:

$$a_{GAM} \sqrt{\sum_{i=1}^{5} d_i^2} + b_{GAM} \sigma_{1,\max} \le \sigma_c , \quad (14)$$

where parameters d_i can be determined from minimum and maximum values of the transformed deviatoric stress tensor:

$$d_i = \frac{1}{2}\left(\max s_i(t) - \max s_i(t)\right), \quad (16)$$

The material parameters a_{GAM} and b_{GAM} are defined as:

$$a_{GAM} = \frac{\kappa-1}{\sqrt{2}\left(1-\frac{1}{\sqrt{3}}\right)} \quad , \quad b_{GAM} = \frac{\sqrt{3}-\kappa}{\sqrt{3}-1} . \quad (17)$$

4 Prediction Criterions Efficiency and Experimental Results

The Fig. 3 shows fatigue life curves and experimental points of sample failure. These curves were drawn according von Mises stress σ_M . It is obvious, that the

specimens with abutment thorn show greater scattering in the graph, which generally reduces prediction effectiveness.

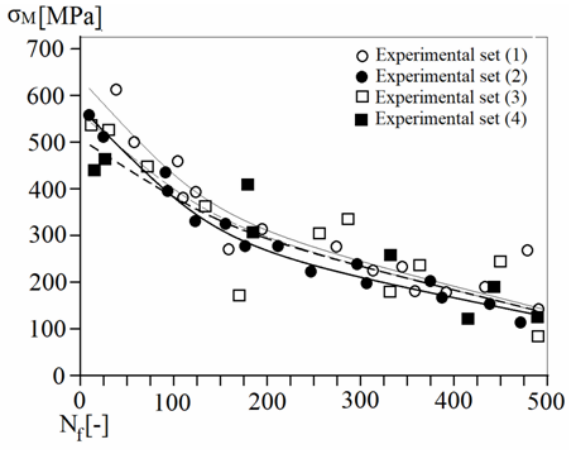

Fig. 3 Fatigue life curves and experimental points of sample failure. The specimens with surface layer thickness 20 nm are marked with black symbol and thick line. The specimens with surface layer thickness 5 nm are marked with empty symbol and thin line. The implants with abutment thorn are recognized by dash line and squares symbols. These curves were drawn according von Mises stress σ_M.

	Error indexes [%]			
Abutment	Screw		Thorn	
Criterion	I_{avr}	$I_{ABS,avr}$	I_{avr}	$I_{ABS,avr}$
GP	-5.83	9.21	-7.43	12.25
GP_{Br}	-0.36	8.78	-3.63	21.49
F	-0.78	9.62	-2.78	10.28
Ma	-0.21	7.32	-1.79	9.68
MD	1.79	8.47	2.72	11.53
Sp	-0.45	8.03	2.90	10.97
PCP	-8.20	17.23	-7.03	16.65
Mr	4.28	8.72	3.76	11.72
S	4.65	12.32	13.65	17.25
C	-3.47	8.65	1.93	12.11
KK	-2.49	8.65	-2.63	13.57
DV	-1.55	8.95	3.37	12.43
PIA	-2.35	8.46	-1.98	10.98
GAM	-2.05	7.93	-1.45	8.12
Ke	-2.39	8.79	-3.11	9.93
ZL	-2.99	8.35	3.21	11.38

Tab. 1 *Average* I_{avr} and absolute average $I_{ABS,avr}$ values of error indexies – thickness of TiO_2 layer 5 nm. Abbreviations are described at the text.

Samples with 20 nm thick surface layer have slightly smaller fatigue resistance than samples with 5 nm thick surface layer. Therefore, it can be said, that the titanium dioxide surface slightly reduces fatigue life, but this effect is negligible. However, the fatigue strength dramatically drops when the peak stress in the cycle reaches the strength of the TiO_2 particles. It is therefore necessary to spread the TiO_2 particles evenly over the surface.

The calculated error indexes are displayed for comparison in Table 1 for samples with surface layer 5 nm and Table 2 for surface layer 20 nm. For all studied criteria were calculated average I_{avr} and absolute average $I_{ABS,avr}$ values of error indexies. Meaning of Abbreviations used in the tables: Gough-Pollard GP; Gough-Pollard for brittle materials GP_{Br}; Findley F; Matake Ma; Marin Mr; Sines S; Crosland C; Dang Van DV; McDiarmid MD; Spagnoli Sp; Gonçalves-Araujo- Mamiya GAM; Kakun-Kawado KK; Keunmegna Ke; Zenner-Liu ZL; Papadopoulos Integral approach PIA; Papadopoulos Critiacal Plane approach PCP.

	Error indexes [%]			
Abutment	Screw		Thorn	
Criterion	I_{avr}	$I_{ABS,avr}$	I_{avr}	$I_{ABS,avr}$
GP	-5.32	8.96	-8.01	13.05
GP_{Br}	-0.36	8.78	-7.37	22.16
F	-0.42	8.63	-1.99	9.86
Ma	-0.43	7.16	-2.31	9.92
MD	1.56	8.13	3.48	13.68
Sp	-0.89	8.69	3.32	13.76
PCP	-8.20	9.21	-4.06	12.35
Mr	3.87	8.43	-4.63	12.62
S	3.98	9.72	13.42	15.23
C	-2.76	8.31	1.32	9.72
KK	-3.09	7.99	-3.27	11.72
DV	-2.11	8.15	-2.63	13.57
PIA	-2.38	8.28	-2.19	9.32
GAM	-2.27	7.65	-1.47	8.56
Ke	-2.79	8. 61	-3.78	10.39
ZL	-3.07	7.98	4.12	12.58

Tab. 1 *Average* I_{avr} and absolute average $I_{ABS,avr}$ values of error indexies – thickness of TiO_2 layer 20 nm. Abbreviations are described at the Table 1.

The comparison of multi-axial criteria data revealed that the Matake criterion was the most successful in the fatigue life prediction for surface abutment screw with 5 nm surface layer. However, the results were much worse in the case implants with abutment thorn. Gonçalves, Araujo and Mamiya criterion gives bests results in this case of implants. Also this criterion gives good results or standard

implant with bolt. Generally, the prediction of fatigue life was much more difficult in the case of thorn abutment, as is evident from the worse results in this case. These results would certainly deserve a more detailed statistical analysis but, the scope of work does not allow this.

If we consider the complex of fatigue prediction criteria and their possible use in professional software for industrial computing, Gonçalves, Araujo and Mamiya criterion can be considered a suitable for utilization in industry [16].

5 Conclusion

The application of titanium dioxide surface leads to small decrease in the fatigue resistance in the low cycle region. So there it is not reason to use resign on this treatment, because there is greater risk for implant failure from biological reason than from the fatigue loading.

The comparison of multiaxial criteria revealed that the Gonçalves, Araujo and Mamiya and Matake criterion are the most successful in the fatigue life prediction of both type of implant. The average value of the error index (taking into account the sign) is the lowest one (I_{avr} = - 2.05). Also the average absolute value of the error index $I_{ABS,avr}{}' = 7.93\,\%$ is very good.

Acknowledgment: This project was prepared by finantial support *"Metoda konečných prvků a automatizace experimentu ve výuce mechaniky a technických laboratoří na katedře technických předmětů"* 18/I zč SV 2119 - Workplace 1440.

References:

[1] H.O. Fuchs, R.L. Stephens, *Metal Fatigue in Engineering*, John Wiley & Sons, Pub., 1980.

[2] Y. Murakami, *Metal Fatigue: Effects of Small Defects and Nonmetallic Inclusions*, Elsevier, 2002.

[3] D.F. Socie, G.B. Marquis, *Multiaxial Fatigue*. Warrendale, 2000.

[4] J.M. Ayllón, C. Navarro, J. Vázquez, J. Domínguez, Fatigue life estimation in dental implants. *Engineering Fracture Mechanics* 123 (2014) pp. 34–43

[5] S. Major S, V. Kocour, P. Cyrus P, Fatigue Life Prediction of Pedicle screw for Spinal Surgery, *Frattura ed Integrita Strutturale*, 10 (2016) 35, pp. 379-388

[6] S. Major, P. Cyrus, M. Hubálovská, The Influence of Surface Roughness on Biocompatibility and Fatigue Life of Titanium Based Alloys**,** *IOP Conf. Series: Materials Science and Engineering* 175, 2017, pp. 1-5

[7] S. Hosseini. Fatigue of Ti-6Al-4V, *Biomedical Engineering - Technical Applications in Medicine*, Dr. Radovan Hudak (Ed.), 2012, pp.75-92.

[8] Mukta Kulkani, Anca Mazare, Patric Schmuki, Ales Iglic. Biomaterial Surface Modification Of Titanium and Titanium Alloys for Medical Applications, *Nanomedicine*, One Central Press, Ed: Alexander Seifalian, Achala de Mel, Deepak M. Kalaskar, 2014, pp.111-136

[9] A. Anders, "*Handbook of Plasma Immersion Ion Implantation and Deposition*." New York: John Wiley & Sons, 2000, pp. 111-136.

[10] I.V. Papadopoulos, P. Davoli, P. Gorla, M. Filippiny, A. Bernasconi, A comparative study of multiaxial high-cycle fatigue criteria for metals, *Int. J. Fatigue* 19, No. 3, 1997, pp. 219-235.

[11] I.V. Papadopoulos, A new criterion fatigue strenght for out-of-phase bending and torsion of hard metals, *Int. J. Fatigue* 16, 1994, pp. 377-384.

[12] A. Carpinteri, A.Spagnoli, Multiaxial high-cycle fatigue criterion for hard metals, *Int. J. Fatigue* 23, 2001, pp. 135-145.

[13] D.L .McDiarmid, A general criterion for high cycle multiaxial fatigue failure, *Fatigue Fracture Engng. Mater. Struct.* 14, No. 4, 1991, pp. 429-453.

[14] D.L .McDiarmid, A shear stress based critical-plane criterion of multiaxial fatigue failure for design and life prediction, *Fatigue Fracture Engng. Mater. Struct.* 17, No. 12, 1994, pp. 1475-1484.

[15] I.V. Papadopoulos, Critical plane approaches in high-cycle fatigue, *Fatigue Fracture Engng. Mater. Struct.* 21 No. 3, 1998, pp. 269-285.

[16] C.A. Gonçalves, J.A. Araujo, E.N. Mamaya, Multiaxial fatigue*:* a stress based criterion for hard metals. *Int. J. Fatigue* 27, 2005, pp. 177-187.

[17] S. Major, S. Hubálovský, V. Kocour, J.Valach, Effectiveness of the Modified Fatigue Criteria for Biaxial Loading Notched Specimen in High-Cycle Region, *Applied mechanics and Materials* Vol.732, 2015, pp. 63-70.